Channel Aware Target Localization With Quantized Data in Wireless Sensor Networks

Onur Ozdemir, *Student Member, IEEE*, Ruixin Niu, *Member, IEEE*, and Pramod K. Varshney, *Fellow, IEEE*

***Abstract*—In this paper, we propose a new maximum-likelihood (ML) target localization approach which uses quantized sensor data as well as wireless channel statistics in a wireless sensor network. The novelty of our approach comes from the fact that statistics of imperfect wireless channels between sensors and the fusion center along with some physical layer design parameters are incorporated in the localization algorithm. We call this approach "channel-aware target localization." ML target location estimators are derived for different wireless channel models and receiver architectures. Furthermore, we derive the Cramér-Rao lower bounds (CRLBs) for our proposed channel-aware ML location estimators. Simulation results are presented to show that the performance of the channel-aware ML location estimators are quite close to their theoretical performance bounds even with relatively small number of sensors and their performance is superior compared to that of the channel-unaware ML estimators.**

***Index Terms*—Cramér-Rao lower bound, imperfect communication channels, target localization, wireless sensor networks (WSNs).**

I. Introduction

With the recent advances in wireless sensor network (WSN) research, applications employing WSNs have become quite popular. Target localization is one of the important applications involving WSNs. A WSN employs low-cost densely deployed sensors that have very limited resources, such as energy and communication bandwidth. They also have limited sensing and communication ranges. Therefore, issues that are related to these limitations and specific to the application have to be resolved before using WSNs in a certain application.

In this paper, we investigate the problem of target localization employing homogeneous low-cost and low-power wireless sensors densely deployed in an area of interest. These sensors report to a fusion center by sending their quantized measurements over wireless channels and the fusion center estimates the position of the target based on received observations. In this framework, there are unavoidable imperfections one can not neglect. First of all, wireless communication channels between sensors and the fusion center are not perfect. Second, sensors have inherent limitations imposed by the current technology in terms of sensing range, computational capability and energy. Some methods have already been developed in the literature to solve target localization problems with networked wireless sensors [4]–[12]. However, to the best of our knowledge, existing localization algorithms do not address both of the above limitations at the same time. In [4]–[8], the signals received by the fusion center are modeled as analog measurements corrupted by white Gaussian noise (WGN). This scheme is not practical for many wireless sensor networks since limited communication within the network is desired to conserve available resources, such as energy and bandwidth. In [9]–[12], target localization methods have been developed based on quantized sensor data assuming perfect communication channels between sensors and the fusion center. Usually, in a target localization scenario, a large number of sensors is deployed in a particular area where a line-of-sight between sensors and the fusion center is not always guaranteed. Therefore, wireless communication is carried out via long-range communication schemes rather than bluetooth or infrared, resulting in lower fidelity. Furthermore, considering the severe resource constraints (energy and bandwidth), each sensor has to transmit a low-power signal at a low data rate to communicate with the fusion center. Error correction coding can be used as a solution to mitigate wireless channel imperfections. However, it results in extra communication overhead which in turn increases energy and bandwidth consumption. Here as an alternative, we focus on developing efficient localization algorithms incorporating the imperfect nature of communication channels as well as based on the constraints of limited resources in a WSN. In this paper we show that, for a given signal-to-noise ratio (SNR) and a given number of sensors, the degradation in the localization performance resulting from nonideal communication channels can be significantly overcome by employing channel-aware data processing at the fusion center.

A generic system model where a number of wireless sensors are employed for target localization is shown in Fig. 1. Sensors receive and process raw measurements, quantize them, and then send quantized measurements via fading and noisy channels to a fusion center. The fusion center fuses the received local sensor measurements using a target localization algorithm to obtain an estimate of the target location. The issue of wireless channel imperfections in the context of distributed detection problems has been investigated in [13]–[19]. However, except for our previous work in [20], wireless channel imperfections in the context of target location estimation have not been analyzed explicitly in the literature. In [20], each channel link between sensors and the fusion center was modeled as an independent hard decoding

Manuscript received December 04, 2007; revised October 28, 2008; accepted October 28, 2008. First published November 21, 2008; current version published February 13, 2009. The associate editor coordinating the review of this manuscript and approving it for publication was Dr. Brian M. Sadler. This work was presented in part at Fusion'07, Quebec City, Canada, July 2007. This work was supported in part by U.S. Army Research Office under award W911 NF-06-1-0250.

The authors are with the Department of EECS, Syracuse University, Syracuse, NY 13244 USA (e-mail: oozdemir@syr.edu; rniu@ecs.syr.edu; varshney@ecs.syr.edu).

Color versions of one or more of the figures in this paper are available online at http://ieeexplore.ieee.org

Digital Object Identifier 10.1109/TSP.2008.2009893

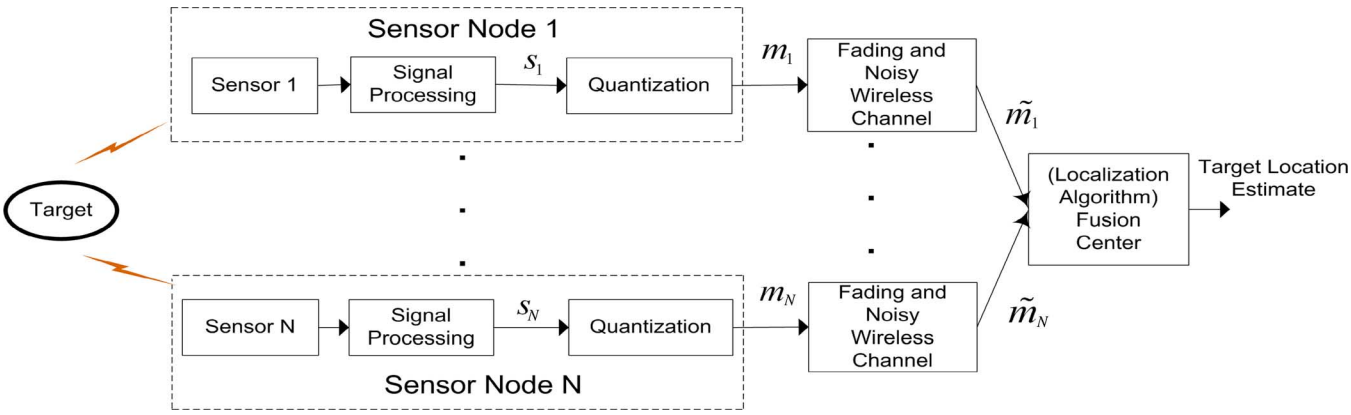

Fig. 1. Generic system model. s_i is the raw sensor measurement of the ith sensor, m_i is the quantized sensor measurement, and $\tilde{m}_i$ is the channel-corrupted sensor measurement received by the fusion center from the ith sensor, where $i = 1, \ldots, N$.

link resulting in a binary symmetric channel (BSC) model. Our goal here is to extend the analysis in [20] to a more general framework where we develop location estimation algorithms and their CRLBs incorporating various physical layer parameters, namely realistic wireless fading channel statistics as well as different reception and decoding strategies. We also evaluate the performance of the proposed target localization algorithms which provides some insights for the design of the physical layer of the network. Furthermore, in order to investigate the robustness of the proposed localization algorithms, we carry out a sensitivity analysis with respect to various possible model mismatches in the system. It is important to note that we incorporate imperfect channel statistics rather than complete instantaneous channel state information (CSI) (instantaneous complex channel gain information [24], or equivalently the instantaneous amplitude and phase of the channel) in our channel-aware target localization algorithms, since the latter may be too costly to determine, especially for a resource constrained WSN. Although our approach is more general than only dealing with channel imperfections, we refer to our developed algorithms as "channel-aware" as they incorporate channel statistics whereas the algorithms which assume perfect channels will be referred to as "channel-unaware" throughout the rest of the paper.

In Section II, the problem of target localization in a WSN is formulated. We derive three different channel-aware ML target localization algorithms along with their corresponding CRLBs in Section III. The first localization algorithm employs a hard-decoding link design and incorporates the bit error probabilities of the channel which is modeled as a binary channel (BC) (note that although BSC is a very general model, it is only a special case of BC), whereas the second and the third localization algorithms are specifically developed for soft-decoding link designs assuming Rayleigh fading channels with phase coherent and phase noncoherent reception, respectively. In Section IV, some simulation results are provided to demonstrate the performance of our developed localization algorithms. We also compare the performance of our algorithms with each other under identical conditions in order to gain some insight about the impact of physical layer on localization performance. Finally, concluding remarks are presented in Section V.

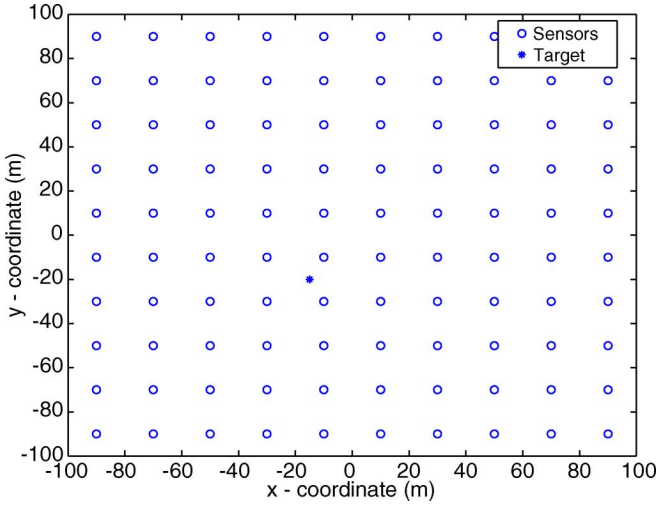

Fig. 2. The target in a grid deployed sensor field.

II. Problem Formulation

As illustrated in Fig. 2, we are interested in localizing a target in a wireless sensor network environment where densely deployed homogeneous and low-cost wireless sensors are employed. All the sensors report to a fusion center which estimates the target location based on local sensor observations. Sensors can be deployed in any manner since our approach is capable of handling any kind of deployment as long as the location information for each sensor is available at the fusion center. However, in this paper, without loss of generality we assume that the sensors are deployed in a grid for simplicity.

The target is assumed to be any source that follows the power attenuation model, such as an acoustic source. We thus use an acoustic signal attenuation model to represent the observed power that is emitted by the target [10]. Our signal attenuation model is based on the fact that an acoustic omnidirectional point source emits signals that attenuate at a rate inversely proportional to the distance from the source if the propagation is through ground surface [1]–[7].

At any given time, the signal power received at a sensor follows a power decay model which is a function of the distance between the target and the sensor:

$$P_i = \frac{P_0 d_0^n}{d_i^n} \tag{1}$$

where P_0 denotes the target signal power at a reference distance of d_0, n is the signal decay exponent which is approximately 2 for detection distances $\leq$1 km [1], [2], and d_i is the distance between the target and the i^{th} sensor

$$d_i = \sqrt{(x_i - x_t)^2 + (y_i - y_t)^2}. \tag{2}$$

Here, (x_i, y_i) and (x_t, y_t) are the coordinates of the i^{th} sensor and the target, respectively. In this paper, without loss of generality, we assume that the reference distance $d_0 = 1$. It is known that for a given acoustic localization scenario, estimates of n can be obtained via experimental data [1]-[2]. In [1], it was verified experimentally that (without wind/turbulence effects and reverberation due to large obstacles) the decay exponent, n, is approximately 2 and this value is assumed in this paper to illustrate the effectiveness of our algorithms. Note also that the acoustic model in (1) is limited to scenarios where wind/turbulence effects are negligible and reverberation due to large obstacles, such as rocky hills and buildings, is minimal [1]–[3], [6], [7]. The fusion center is assumed to know the locations of the sensors. At each sensor, the received signal amplitude is given by

$$s_i = a_i + n_i \tag{3}$$

where $a_i = \sqrt{P_i}$ is the true measurement corrupted by the noise term, n_i, modeled as additive white Gaussian noise (AWGN), i.e., $n_{ik} \sim \mathcal{N}(0, \sigma_n^2)$, which represents the cumulative effects of sensor background noise and the modeling error of acoustic signal parameters. We assume that sensor noises n_i as well as wireless links between the sensors and the fusion center are independent across sensors, and σ_n^2 is known. Note that the noise statistics can also be empirically determined for a specific application. The sensor signal model given in (3) results from averaging time samples of the received acoustic energy. The interested reader is referred to [1], [3], [6], [7] for the details. Although it is not a requirement for our approach to work, the sensors are assumed to have identical noise variances for simplicity. At each sensor, the received signal is quantized before being sent to the fusion center. Quantization is done locally at the sensors in order to decrease the communication burden on the sensors thereby reducing energy consumption. The quantized observation model at sensor i is the following:

$$m_i = \begin{cases} 0, & \gamma_{i0} < s_i < \gamma_{i1} \\ 1, & \gamma_{i1} < s_i < \gamma_{i2} \\ \vdots & \vdots \\ L-1, & \gamma_{i(L-1)} < s_i < \gamma_{iL}. \end{cases} \tag{4}$$

Here, m_i is the quantized measurement of the i^{th} sensor and $\gamma_{i0}, \ldots, \gamma_{iL}$ are the predetermined thresholds for a $K = log_2 L$ bit quantizer. Note that $\gamma_{i0} = -\infty$ and $\gamma_{iL} = \infty$. Based on (4), the transmitted observations from sensors to the fusion center can be denoted in vector form as $\mathbf{M} = [m_1\ m_2\ \ldots\ m_N]^T$, where the superscript T denotes the transpose operation and N is the total number of sensors deployed in the area of interest. Here, $\theta = [P_0\ x_t\ y_t]^T$ is the parameter vector that needs to be estimated. Using the sensor observation model in (3) with the Gaussian noise assumption and the quantization model in (4), it is easy to derive $p(m_i|\theta)$, the probability of a quantized sensor measurement taking a specific value conditioned on the target location:

$$p(m_i|\theta) = \begin{cases} Q\left(\frac{\gamma_{i0}-a_i}{\sigma_n}\right) - Q\left(\frac{\gamma_{i1}-a_i}{\sigma_n}\right), & m_i = 0 \\ Q\left(\frac{\gamma_{i1}-a_i}{\sigma_n}\right) - Q\left(\frac{\gamma_{i2}-a_i}{\sigma_n}\right), & m_i = 1 \\ \vdots & \vdots \\ Q\left(\frac{\gamma_{i(L-1)}-a_i}{\sigma_n}\right) - Q\left(\frac{\gamma_{iL}-a_i}{\sigma_n}\right), & m_i = L-1 \end{cases} \tag{5}$$

where $Q(\cdot)$ is the complementary distribution function of the standard Gaussian distribution defined as

$$Q(x) = \int_x^\infty \frac{1}{\sqrt{2\pi}} e^{-\frac{t^2}{2}} dt. \tag{6}$$

If one neglects the effects of unreliable wireless channels between sensors and the fusion center, then the fusion center could be assumed to receive an exact replica of $\mathbf{M}$ in order to perform the assigned task, which is location estimation in this paper. However, this assumption is not always valid for a WSN because of the reasons explained in Section I, i.e., the channels between wireless sensors and the fusion center are unreliable. Let $\mathbf{Y}$ denote the observation vector at the fusion center after transmission through the imperfect channels

$$\mathbf{Y} = [\tilde{m}_1 \quad \tilde{m}_2 \quad \ldots \quad \tilde{m}_N]^T \tag{7}$$

where $\tilde{m}_i$s are the quantized sensor measurements corrupted by the imperfect wireless channels. The fusion center needs to estimate the source location based on $\mathbf{Y}$.

III. Location Estimation Based on Channel Statistics

For a WSN, one has the flexibility to design the communication link layer and different design choices result in different performance in terms of location estimation accuracy. The functions of the link layer that need to be designed include modulation schemes, data encryption techniques, transceiver architectures and decoding schemes at the receiver. In this section, we assume that the channel model is fixed and analyze different decoding strategies at the fusion center. There are two different link layer designs that can be utilized depending on the decoding scheme at the fusion center. The fusion center can either make a hard decision for each bit before performing the localization task or use received measurements directly to estimate the location. The former and the latter link layer designs are called hard-decoding link and soft-decoding link, respectively. Given a hard-decoding link, if the communication channel statistics and the parameters of the network physical layer are known, the probability of making a wrong decision can be calculated and the corresponding channel can be modeled as a binary-channel (BC). We analyze the system assuming BCs for hard-decoding links. As for the soft-decoding links, we assume Rayleigh flat

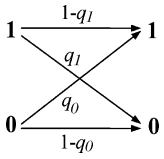

Fig. 3. Binary channel.

fading channels between sensors and the fusion center, and further consider two different reception techniques which are phase coherent and phase noncoherent reception. The former reception technique requires phase information of the received signal whereas the latter does not, and depending on the reception technique, different sensor signaling schemes need to be adopted. The tradeoffs between these two reception techniques will be discussed in the next section. Given a WSN, the assumption of Rayleigh flat fading channels is quite reasonable because of homogeneous scattering background and operation at short ranges with low duty cycles (energy and bandwidth constraints) [16]. Note that for a soft-decoding link, both the knowledge of the channel statistics and the physical layer parameters need to be incorporated directly in the localization algorithm since no hard decision is made beforehand.

To summarize, we develop three different target location estimation algorithms and derive their performance bounds (CRLBs) for three different link layer designs, namely, the BC, Rayleigh fading channel with coherent reception, and Rayleigh fading channel with noncoherent reception.

A. Hard-Decoding Binary Channel (BC)

A general binary channel model with bit error probabilities q_0 and q_1 is shown in Fig. 3. It is easy to see that the received observation models at the fusion center are dependent on the channel statistics, i.e., on q_0 and q_1. Here, we assume, for simplicity, that each channel between the sensors and the fusion center has identical bit error probabilities and channel links are independent of each other. However, note that our methodology will still work for more general BC models, i.e., even if different channels have different bit error probabilities.

Using the channel model in Fig. 3, the probability of a received sensor observation $\tilde{m}_i$ taking a specific value m, given the target location, can be written as

$$p(\tilde{m}_i = m|\theta) = \sum_{m_i=0}^{L-1} p(\tilde{m}_i = m|m_i)p(m_i|\theta) \tag{8}$$

where the result $p(\tilde{m}_i|m_i,\theta) = p(\tilde{m}_i|m_i)$, due to the fact that θ, m_i and $\tilde{m}_i$ form a Markov chain, has been used. Note that channel statistics is represented by the first term in the summation in (8). For example, given a target location θ, if $L = 2$ is used to send the measurements through a BC, the probability of a received observation from sensor i being equal to 1 is $p(\tilde{m}_i = 1|\theta) = p(m_i = 1|\theta)(1 - q_1) + p(m_i = 0|\theta)q_0$. For $L > 2$, the channel statistics depend on whether a bit-by-bit or a symbol-by-symbol decoding is carried out at the receiver. In this paper, without loss of generality, we assume that the decoding at the receiver is done on a bit-by-bit basis as also described in Section IV-A. Since sensor noises and wireless links are assumed to be independent, the likelihood function at the fusion center can be written as

$$\begin{aligned} p(\mathbf{Y}|\theta) &= \prod_{i=1}^{N} p(\tilde{m}_i|\theta) \\ &= \prod_{i=1}^{N} \left[\sum_{m_i=0}^{L-1} p(\tilde{m}_i|m_i)p(m_i|\theta) \right]. \end{aligned} \tag{9}$$

Using (9), it is straightforward to derive the log-likelihood function of $\mathbf{Y}$,

$$\ln p(\mathbf{Y}|\theta) = \sum_{i=1}^{N} \ln \left[\sum_{m_i=0}^{L-1} p(\tilde{m}_i|m_i)p(m_i|\theta) \right]. \tag{10}$$

The ML target location estimator, $\hat{\theta}$, is now the solution of the following maximization problem:

$$\hat{\theta} = \arg\max_{\theta} \ln p(\mathbf{Y}|\theta). \tag{11}$$

Note that the only parameters the fusion center needs to know in order to localize the target are the received signal decay model, the sensor locations and the binary channel statistics, i.e., q_0 and q_1. All of these parameters can be predetermined by performing off-line experiments. If coherent reception is employed at the fusion center, the receiver needs to estimate the channel phase only. Channel gain does not need to be estimated. As for the noncoherent reception case, the receiver does not need to estimate neither the channel phase nor the channel gain. Therefore, in either reception scenario, there is no need to determine complete instantaneous CSI for each received signal in order to perform the localization task. The Cramér-Rao lower bound (CRLB) for this estimation problem is obtained and stated in the following theorem.

Theorem 1: For any unbiased estimator $\hat{\theta}(\mathbf{Y})$, the CRLB is given by

$$E\left\{ \left[\hat{\theta}(\mathbf{Y}) - \theta \right] \left[\hat{\theta}(\mathbf{Y}) - \theta \right]^T \right\} \geq \mathbf{F}^{-1} \tag{12}$$

in which $\mathbf{F}$ is the Fisher information matrix (FIM) given for the BC as follows:

$$\mathbf{F} = \sum_{i=1}^{N} \sum_{\tilde{m}_i=0}^{L-1} \frac{\nabla_\theta p(\tilde{m}_i|\theta) \nabla_\theta^T p(\tilde{m}_i|\theta)}{p(\tilde{m}_i|\theta)} \tag{13}$$

where the term $p(\tilde{m}_i|\theta)$ is given in (8). The operator ∇ in (13) is the gradient operator expressed as

$$\nabla_\theta = \left[\frac{\partial}{\partial P_0} \; \frac{\partial}{\partial x_t} \; \frac{\partial}{\partial y_t} \right]^T. \tag{14}$$

The expression for the gradient term in (13) is

$$\nabla_\theta p(\tilde{m}_i|\theta) = \sum_{m_i=0}^{L-1} p(\tilde{m}_i|m_i) \nabla_\theta p(m_i|\theta) \tag{15}$$

in which

$$\begin{aligned}\frac{\partial p(m_i=l|\theta)}{\partial P_0} &= \frac{d_i^{-\frac{n}{2}}\lambda_{il}}{2\sqrt{2\pi}\sigma_n\sqrt{P_0}}\\ \frac{\partial p(m_i=l|\theta)}{\partial x_t} &= \frac{na_i d_i^{-2}(x_i-x_t)\lambda_{il}}{2\sqrt{2\pi}\sigma_n}\\ \frac{\partial p(m_i=l|\theta)}{\partial y_t} &= \frac{na_i d_i^{-2}(y_i-y_t)\lambda_{il}}{2\sqrt{2\pi}\sigma_n}\end{aligned} \tag{16}$$

and

$$\lambda_{il} = \left[e^{-\frac{(\gamma_{il}-a_i)^2}{2\sigma_n^2}} - e^{-\frac{\left(\gamma_{i(l+1)}-a_i\right)^2}{2\sigma_n^2}}\right]. \tag{17}$$

Proof: See Appendix A. ∎

The CRLBs for the target signal power and the target location coordinates, P_0, x_t and y_t, are the diagonal elements of the inverse FIM, respectively, i.e.

$$\begin{aligned}var(\hat{P}_0) &\geq \left[\mathbf{F}^{-1}(\theta)\right]_{11},\\ var(\hat{x}_t) &\geq \left[\mathbf{F}^{-1}(\theta)\right]_{22},\\ var(\hat{y}_t) &\geq \left[\mathbf{F}^{-1}(\theta)\right]_{33}.\end{aligned} \tag{18}$$

B. Soft-Decoding in Rayleigh Fading Channel With Coherent Reception

Here, we consider a discrete-time Rayleigh flat fading channel with a stationary and ergodic complex gain of $h_i e^{j\phi_i}$ between the ith sensor and the fusion center. Note that h_i and ϕ_i denote the fading envelope and the phase of the channel, respectively. It is assumed that the channel gain remains constant during a symbol transmission and channels are independent of each other. We further simplify the analysis by assuming binary signaling ($L = 2$) and replace $\{0,1\}$ by $\{-1,1\}$ in (4), so that the effect of the fading channel reduces to a real scalar multiplication for phase coherent reception [16]. This is illustrated by using the received signal model for sensor i

$$\tilde{r}_i = h_i e^{j\phi_i} m_i + v_i \tag{19}$$

where v_i is a zero-mean complex Gaussian noise with independent real and imaginary parts having identical variance σ_v^2, i.e., $v_i \sim \mathcal{CN}(0, 2\sigma_v^2)$. Note that the notation $\mathcal{CN}$ represents complex Gaussian distribution. Without loss of generality, we make the assumption of Rayleigh fading channels with unit power, i.e., $h_i e^{j\phi_i} \sim \mathcal{CN}(0,1)$, therefore $E[h_i^2] = 1$. Using the knowledge of the channel phase at the receiver, the observation model at the fusion center for the ith sensor can be obtained as

$$\tilde{m}_i = Re\{\tilde{r}_i e^{-j\phi_i}\} = h_i m_i + Re\{v_i e^{-j\phi_i}\}. \tag{20}$$

Since v_i follows a circularly symmetric complex Gaussian distribution, the noise term in (20) is real WGN with variance σ_v^2, i.e., $Re\{v_i e^{-j\phi_i}\} \sim \mathcal{N}(0, \sigma_v^2)$. With the unit power Rayleigh fading channel assumption, the probability density function (PDF) of h_i is given as:

$$p(h_i) = 2h_i e^{-h_i^2}, \quad h_i \geq 0. \tag{21}$$

Then, it is straightforward to obtain the conditional PDF $p(\tilde{m}_i|m_i)$, i.e., the PDF of the transmitted signal $\tilde{m}_i$ given sensor observation m_i:

$$p(\tilde{m}_i|m_i) = \int_0^\infty p(\tilde{m}_i|h_i, m_i)p(h_i)dh_i. \tag{22}$$

Following the above assumptions and the same procedure, the conditional PDF $p(\tilde{m}_i|m_i)$ has already been derived in [16] and given as follows:

$$\begin{aligned}p(\tilde{m}_i|m_i) &= \frac{2\sigma_v}{\sqrt{2\pi}\,(1+2\sigma_v^2)}\\ &\quad\times e^{\frac{-\tilde{m}_i^2}{2\sigma_v^2}}\left[1 + m_i\sqrt{2\pi}\alpha\tilde{m}_i e^{\frac{(\alpha\tilde{m}_i)^2}{2}} Q(-\alpha m_i\tilde{m}_i)\right]\end{aligned} \tag{23}$$

where $\alpha = 1/(\sigma_v\sqrt{1+2\sigma_v^2})$. Then, it is easy to obtain

$$p(\tilde{m}_i|\theta) = \sum_{m_i\in\{-1,1\}} p(\tilde{m}_i|m_i)p(m_i|\theta) \tag{24}$$

where the terms in the summation are given in (23) and (5), respectively.

Following the same procedure as in the previous section, the log-likelihood function of $\mathbf{Y}$ as well as the corresponding ML estimator of the target location, $\hat{\theta}$, can be derived as follows:

$$\ln p(\mathbf{Y}|\theta) = \sum_{i=1}^{N} \ln\left[\sum_{m_i\in\{-1,1\}} p(\tilde{m}_i|m_i)p(m_i|\theta)\right] \tag{25}$$

$$\hat{\theta} = \arg\max_\theta \ln p(\mathbf{Y}|\theta). \tag{26}$$

In this case, the fusion center needs to estimate the phase of the received signal in addition to the required knowledge about the received signal decay model, the sensor locations and the Rayleigh fading channel statistics. Note that for a given surveillance environment, fading channel statistics can be derived off-line via experimental data [22]. Details and discussions about how to obtain wireless channel statistics can be found in [22]. Incorporation of the Rayleigh fading channel statistics into the localization algorithm eliminates the need for estimating instantaneous channel gain, h_i, for each received signal. The CRLB for this estimation problem is also obtained and stated in the following theorem.

Theorem 2: For any unbiased estimator $\hat{\theta}(\mathbf{Y})$, the CRLB is given by $E\{[\hat{\theta}(\mathbf{Y}) - \theta][\hat{\theta}(\mathbf{Y}) - \theta]^T\} \geq \mathbf{F}^{-1}$ in which $\mathbf{F}$ is the FIM and it is given for the Rayleigh fading channel with coherent reception as follows:

$$\mathbf{F} = \sum_{i=1}^{N}\int_{-\infty}^{\infty} \frac{\nabla_\theta p(\tilde{m}_i|\theta)\nabla_\theta^T p(\tilde{m}_i|\theta)}{p(\tilde{m}_i|\theta)} d\tilde{m}_i. \tag{27}$$

The expression for the gradient term in (27) is

$$\nabla_\theta p(\tilde{m}_i|\theta) = \sum_{m_i \in \{-1,1\}} p(\tilde{m}_i|m_i) \nabla_\theta p(m_i|\theta), \tag{28}$$

where the conditional PDF $p(\tilde{m}_i|m_i)$ and the partial derivative terms are given in (23) and (16), respectively.

Proof: See Appendix B. ∎

It should be mentioned that closed forms for the integrals in (27) do not exist. Therefore, numerical integration methods are needed for evaluating the elements of the FIM.

C. Soft-Decoding in Rayleigh Fading Channel With Noncoherent Reception

Assuming the same wireless channel conditions and binary signaling as in Section III-B, here we analyze our third link layer design scenario where phase noncoherent reception is employed at the fusion center. We assume that energy detection (ED) is employed at the receiver as it is a low-cost and widely used noncoherent detection scheme [23]. Therefore, for a binary signaling scheme, it is natural to utilize ON/OFF signaling at the sensors where they remain silent for $m_i = 0$. Therefore, unlike the coherent reception case in Section III-B, we return to $m_i \in \{0,1\}$ rather than $\{-1,1\}$. Then the received signal model for sensor i before ED is given as

$$r_i = \begin{cases} v_i, & m_i = 0 \\ h_i e^{j\phi_i} + v_i, & m_i = 1 \end{cases} \tag{29}$$

where $v_i \sim \mathcal{CN}(0, 2\sigma_v^2)$, and $h_i e^{j\phi_i} \sim \mathcal{CN}(0,1)$ (unit power Rayleigh fading channel). After ED, the observation model at the fusion center for the ith sensor is simply $\tilde{m}_i = |r_i|^2$, where $|\cdot|$ indicates the magnitude of a complex number. Then, it is easy to obtain the conditional PDF

$$\begin{aligned} p(\tilde{m}_i|m_i = 0) &= \frac{1}{2\sigma_v^2} e^{-\frac{\tilde{m}_i}{2\sigma_v^2}} \\ p(\tilde{m}_i|m_i = 1) &= \frac{1}{1+2\sigma_v^2} e^{-\frac{\tilde{m}_i}{1+2\sigma_v^2}}. \end{aligned} \tag{30}$$

Similar to the previous section, the conditional PDF $p(\tilde{m}_i|\theta)$ can be written as

$$p(\tilde{m}_i|\theta) = \sum_{m_i=0}^{1} p(\tilde{m}_i|m_i) p(m_i|\theta). \tag{31}$$

The same analysis as in the previous two sections can be applied here to find the log-likelihood function of $\mathbf{Y}$ and the corresponding ML estimator of the target location $\hat{\theta}$

$$\ln p(\mathbf{Y}|\theta) = \sum_{i=1}^{N} \ln \left[\sum_{m_i=0}^{1} p(\tilde{m}_i|m_i) p(m_i|\theta) \right] \tag{32}$$

$$\hat{\theta} = \arg\max_\theta \ln p(\mathbf{Y}|\theta). \tag{33}$$

Note that in this case, the fusion center does not need to estimate the phase of the received signal. The only parameters the fusion center need to know are the received signal decay model, the sensor locations and the Rayleigh fading channel statistics. Therefore, instantaneous CSI need not be determined. The CRLB for this estimation problem is also obtained and stated in the following theorem.

Theorem 3: For any unbiased estimator $\hat{\theta}(\mathbf{Y})$, the CRLB is given by $E\{[\hat{\theta}(\mathbf{Y}) - \theta][\hat{\theta}(\mathbf{Y}) - \theta]^T\} \geq \mathbf{F}^{-1}$ in which $\mathbf{F}$ is the FIM and it is given for the Rayleigh fading channel with noncoherent reception as follows:

$$\mathbf{F} = \sum_{i=1}^{N} \int_0^\infty \frac{\nabla_\theta p(\tilde{m}_i|\theta) \nabla_\theta^T p(\tilde{m}_i|\theta)}{p(\tilde{m}_i|\theta)} d\tilde{m}_i. \tag{34}$$

The expression for the gradient term in (34) is

$$\nabla_\theta p(\tilde{m}_i|\theta) = \sum_{m_i=0}^{1} p(\tilde{m}_i|m_i) \nabla_\theta p(m_i|\theta) \tag{35}$$

where the conditional PDF $p(\tilde{m}_i|m_i)$ and the partial derivative terms are given in (30) and (16), respectively.

Proof: See Appendix C. ∎

As in the previous section, closed forms for the integrals in (34) do not exist. Therefore numerical integration methods are needed for evaluating the elements of the FIM.

IV. Performance Evaluation

In this section, we provide some simulation results to assess the performance of our channel aware target localization approach developed in Section III, for three different link layer designs. Sensors are assumed to be grid deployed in a 200 m × 200 m area as shown in Fig. 2. Target is assumed to be located at $(x_t, y_t) = (10, 20)$ and $P_0 = 25000$ is used as the target signal power defined in (1), i.e., $\theta = [25000\ 10\ 20]^T$. Note that depending on the choice of sensor locations and the target parameter vector, θ, resulting CRLBs and therefore the localization performance will be different since CRLBs are functions of both the target parameters and the sensor locations. For simplicity, each sensor is assumed to employ identical thresholds for quantization, hence the sensor index i is omitted in γ_{il}. We also assume that sensor background noise has unit power, i.e. $\sigma_n^2 = 1$.

The evaluations of integrals in (27) and (34) for CRLB calculations are carried out using composite Simpson's rule [25]. For the maximization of the likelihood functions, a two-step procedure is adopted in order to minimize the risk of converging to a local maximum. We first perform a coarse grid search within the surveillance region and a reasonable interval of target signal power P_0 to find an approximate maximum point. This point is then used to initialize a simplex search algorithm provided by MATLAB to perform the final maximization.

First, in Section IV-A, we evaluate the performance of our channel-aware location estimation algorithm assuming hard-decoding links and imperfect channel conditions, namely BCs, and perform a comparison with the existing channel-unaware location estimation algorithm which assumes hard decoding links with perfect channel conditions. For simplicity, we further assume that probability of making a wrong decision for each bit is identical, i.e., bit-error-rate (BER)$= q_0 = q_1$, forming a BSC model. Second, in Section IV-B, we evaluate the performance of our channel-aware location estimators assuming soft-decoding links (coherent and noncoherent) and show the performance gains by employing the soft-decoding receiver

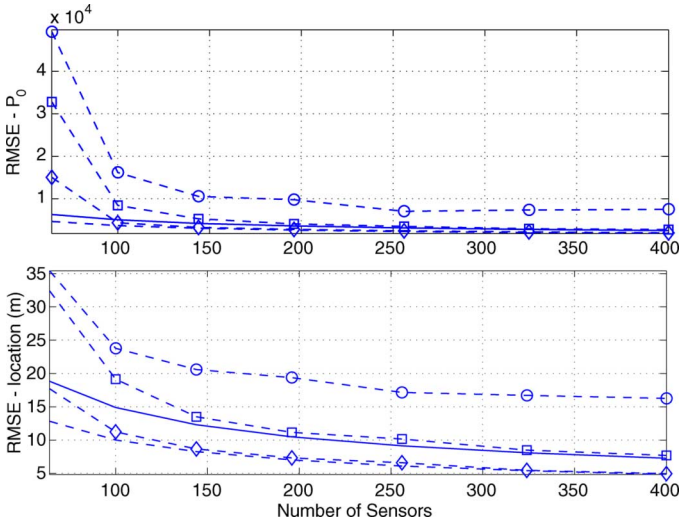

Fig. 4. RMS errors of channel-aware and channel-unaware ML estimation methods using binary data compared to their theoretical CRLB in meters. Dash: channel-unaware CRLB with perfect channels, dash-diamond: channel-unaware ML with perfect channels, solid line: channel-aware CRLB with imperfect channels, dash-square: channel-aware ML with imperfect channels, dash-circle: channel-unaware ML with imperfect channels (BER $q_0 = q_1 = 0.1$ for imperfect channel cases, $(x_t, y_t) = (10, 20), \gamma_1 = 1.7$).

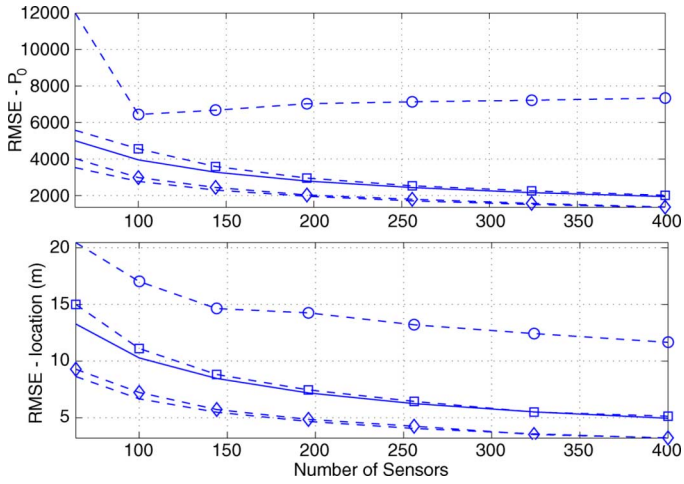

Fig. 5. RMS errors of channel-aware and channel-unaware ML estimation methods using quaternary data compared to channel-aware CRLB in meters. Dash: channel-unaware CRLB with perfect channels, dash-diamond: channel-unaware ML with perfect channels, solid line: channel-aware CRLB with imperfect channels, dash-square: channel-aware ML with imperfect channels, dash-circle: channel-unaware ML with imperfect channels ($q_0 = q_1 = 0.1, (x_t, y_t) = (10, 20), \gamma_1 = 0.82, \gamma_2 = 1.7, \gamma_3 = 2.72$).

architecture. Note that without obtaining CSI, it is impossible to employ channel-unaware target localization algorithms using a soft-decoding scheme since soft-decoding requires the use of channel statistics; this is another advantage gained by incorporating channel statistics in the localization algorithm. In Section IV-C, we investigate the effects of link-layer designs on localization performance. Finally, in Section IV-D we carry out a sensitivity analysis of our developed algorithms to errors in prior information for various system parameters.

A. Binary Symmetric Channel (BSC)

Note that the error probability for each transmitted bit is identical for a BSC, i.e., $q_0 = q_1$. Fig. 4 depicts both the motivation behind our channel-aware target localization approach and the significant performance gain achieved by this approach. First, we demonstrate two different scenarios in which we investigate the performance of the channel-unaware ML estimator which assumes that the communication channels are perfect, i.e., $q_0 = q_1 = 0$. In other words, the channel-unaware ML estimator does not incorporate channel statistics information at all, which is the case for the estimators developed in the literature so far. In the first scenario, all the channels are modeled as perfect whereas in the second scenario the channels are modeled as BSCs with bit BERs equal to 0.1. Note that details about quantization threshold design along with some robust approaches can be found in [10]. Throughout our simulations, we have used the same quantization thresholds as those used in [10].

In Fig. 4, the performance of the channel-unaware ML estimator using binary data for these two different scenarios is shown as a function of the number of sensors employed, N. CRLB for the channel-unaware ML estimator (channel-unaware CRLB) is also provided as a performance measure. Since binary data is used, there is only one threshold, γ_1, and it is set to 1.7 for the 1-bit quantization [10]. Root mean square (RMS) error is used as the performance criterion and each RMS value is computed based on 1000 Monte-Carlo trials. As is clearly seen in Fig. 4, the channel-unaware ML estimator has significant performance degradation for the scenario when channels are not perfect. This result is the main motivation behind our work in this paper. As a second demonstration in Fig. 4, the performance of the channel-aware ML estimator using binary data is compared with its theoretical CRLB as a function of the number of sensors, N. All the parameters are kept the same as those used in the channel unaware scenarios. It is clearly seen that as the number of sensors increases, the performance of the channel-aware ML estimator improves and converges to the CRLB. Even when the number of sensors is relatively small, the performance of the ML estimator is quite close to the CRLB. It is also obvious that the performance of the channel-aware ML estimator is much better compared to the channel-unaware ML estimator when channels are imperfect. Furthermore, the channel-aware CRLB provides a much tighter performance bound for the target location estimation problem with imperfect channels. To summarize, we were able to move the performance towards that of the ideal perfect channel case via channel-aware processing as seen in Fig. 4.

In Fig. 5, the performance of the channel-aware ML estimator using quaternary data, i.e., $L = 4$, is compared with the theoretical CRLB as a function of the number of sensors employed. For this scenario, we assume that the decoding at the receiver is done on a bit-by-bit basis forming a channel model where two BSCs are used in parallel. All the parameters except quantization thresholds are kept the same as the case for Fig. 4. Quantization thresholds for the quaternary data are identical for each sensor and they are set to 0.82, 1.7, and 2.72, respectively, [10]. Very similar to the case in Fig. 4, the performance of the channel-aware ML estimator improves very quickly and converges to the CRLB as N increases. In addition, the performance of the channel-aware ML estimator is extremely close to CRLB even when the amount of data is relatively small. Channel-aware

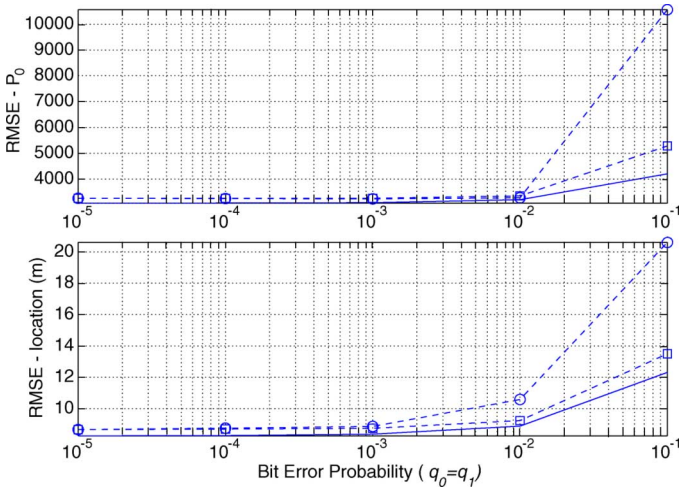

Fig. 6. RMS errors of channel-aware and channel-unaware ML estimation methods using binary data compared to channel-aware CRLB in meters with respect to different bit error probabilities. Solid line: channel-aware CRLB, dash-square: channel-aware ML, dash-circle: channel-unaware ML ($\mathrm{N} = 144$, $(x_t, y_t) = (10, 20)$).

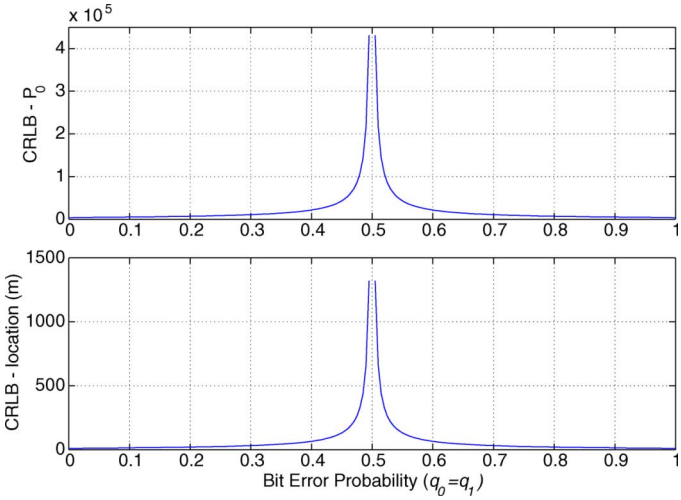

Fig. 7. CRLB as a function of bit error probability ($\mathrm{N} = 100$, $(x_t, y_t) = (10, 20)$).

processing again allows us to move towards the ideal perfect channel case as seen in Fig. 5. Note also that the performance of the channel-aware ML estimator using quaternary data is better compared to that using binary data as expected since the former provides more information about the target location.

Next, the performances of channel-aware and channel-unaware ML estimators are compared for different bit error probabilities, p in Fig. 6. In this case, both estimators use binary data to estimate the target location and the number of sensors, N is set to 144. As can be seen in the figure, the performance of the channel-unaware ML estimator degrades significantly as the channel gets worse, i.e., as q_0 and q_1 increase. However, the performance of the channel-aware ML estimation approach is quite robust to imperfections of the wireless channels since channel statistics has been included in the estimation process.

Fig. 7 shows CRLBs for the channel-aware ML estimator using binary data with respect to the complete range of possible bit-error probabilities. The CRLB approaches infinity as $q_0 \rightarrow 0.5$ and approaches its minimum as $q_0 \rightarrow 0$ and $q_0 \rightarrow 1$. This is an expected result since the CRLB is computed assuming perfect knowledge of channel statistics at the fusion center. As $q_0 \rightarrow 0.5$, the channels are completely random and there is much larger uncertainty. As $q_0 \rightarrow 0$ and $q_0 \rightarrow 1$, the channel becomes less uncertain resulting in smaller CRLB values.

B. Rayleigh Fading Channel

Similar to the previous section, we evaluate the performance of our channel-aware target localization algorithms developed for Rayleigh fading soft-decoding links by comparing them with their theoretical CRLBs. Fig. 8 shows RMS errors of target location estimates based on 1000 Monte Carlo trials along with their corresponding CRLBs as a function of the number of sensors, for phase coherent and phase noncoherent reception scenarios. Both simulations are performed assuming unit power Rayleigh fading channels, i.e., $E[h_i^2] = 1$, and the same average

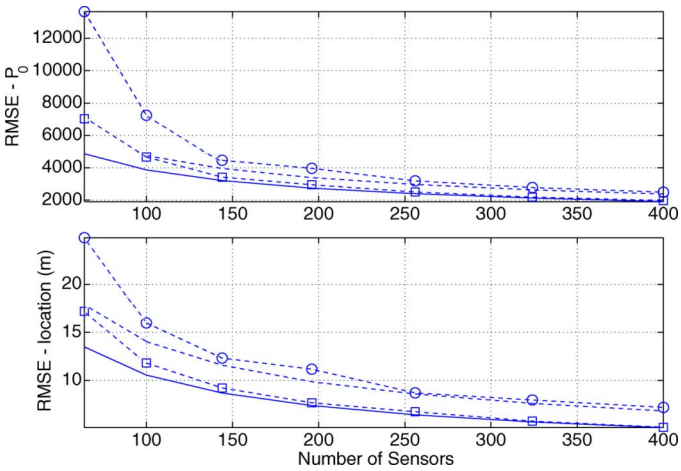

Fig. 8. RMS errors of channel-aware ML estimation methods for Rayleigh fading channel with coherent and noncoherent receptions compared to channel-aware CRLBs in meters. Solid line: channel-aware CRLB for coherent reception, dash-square: channel-aware ML for coherent reception, dash: channel-aware CRLB for noncoherent reception, dash-circle: channel-aware ML for noncoherent reception (Channel $\mathrm{SNR} = 10$ dB, $(x_t, y_t) = (10, 20)$).

channel SNR which is 10 dB. Note that the coherent reception scenario employs antipodal signaling with unit amplitude ($m_i \in \{-1, 1\}$) whereas the noncoherent reception scenario employs ON/OFF signaling ($m_i \in \{0, 1\}$). As is clearly seen from the figure, similar to the BSC scenario, channel-aware target location estimators for soft-decoding links achieve their CRLBs using relatively small number of sensors. For the same channel SNR and the same number of sensors, the localization performance of the noncoherent receiver is worse than that of the coherent receiver since the latter incorporates phase information of the received signal. Here, the tradeoff is the need for the exact knowledge of the phase of the channel resulting in extra energy consumption and the complexity of the receiver since noncoherent ED does not need any phase information and requires a low-cost and simpler receiver architecture compared to existing phase-coherent receivers.

C. Comparison of Link Layer Designs

To better understand the effect of link layer design on localization performance, different link layer design schemes need to be compared under identical channel conditions. The link layer designs we compare are 1) Rayleigh fading coherent soft-decoding link with channel-aware processing, 2) Rayleigh fading noncoherent soft-decoding link with channel-aware processing, 3) Rayleigh fading coherent hard-decoding link with channel-aware processing, 4) Rayleigh fading coherent hard-decoding link with channel-unaware processing, 5) Rayleigh fading noncoherent hard-decoding link with channel-aware processing and 6) Rayleigh fading noncoherent hard-decoding link with channel-unaware processing. Note that the type of the localization algorithm employed at the fusion center is also assumed to be a part of the link layer design parameter for comparison purposes. It is assumed that binary signaling is employed for all scenarios. Note that as long as channel statistics are known, any hard-decoding link can be modeled as a BC by deriving its corresponding bit error probabilities as a function of average channel SNR. Then, the localization algorithm developed in Section III-A can be utilized to evaluate the performance. Therefore, given a particular communication channel, in order to perform a comparison between hard-decoding links and soft-decoding links, the corresponding bit error probabilities need to be derived to be used in the localization algorithm for the hard-decoding link, i.e., the corresponding BC link. It is shown in [23] that for antipodal signaling (BPSK), where $m_i = \pm A$, hard-decoding link forms a binary symmetric channel (BSC) and the error probability P_e for the corresponding fading channel is given as

$$P_e = \frac{1}{2}\left(1 - \sqrt{\frac{SNR}{1+SNR}}\right) \tag{36}$$

where $SNR = (A^2/N_0)\overline{h^2}$ and $N_0/2$ is the power spectral density (PSD) of the additive noise. The expression in (36) can be used to calculate the BER as a function of SNR for Rayleigh fading coherent hard-decoding links. In addition, we derive P_e for a Rayleigh fading noncoherent hard-decoding link using ON/OFF signaling and state it in the following lemma.

Lemma 1: For ON/OFF signaling scheme, where either $m_i = 0$ or $m_i = B$ is transmitted, the error probability is given by

$$\begin{aligned} P_e &= \frac{1}{2}\left[P(\textit{decide } B|m_i = 0) + P(\textit{decide } 0|m_i = B)\right] \\ &= \frac{1}{2}\left[1 - \frac{2SNR}{(2SNR+1)^{\frac{2SNR+1}{2SNR}}}\right] \end{aligned} \tag{37}$$

where

$$P(\textit{decide } B|m_i = 0) = \left(\frac{1}{2SNR+1}\right)^{\frac{2SNR+1}{2SNR}} \tag{38}$$

$$P(\textit{decide } 0|m_i = B) = 1 - \left(\frac{1}{2SNR+1}\right)^{\frac{1}{2SNR}} \tag{39}$$

and $SNR = (B^2/2N_0)\overline{h^2}$.

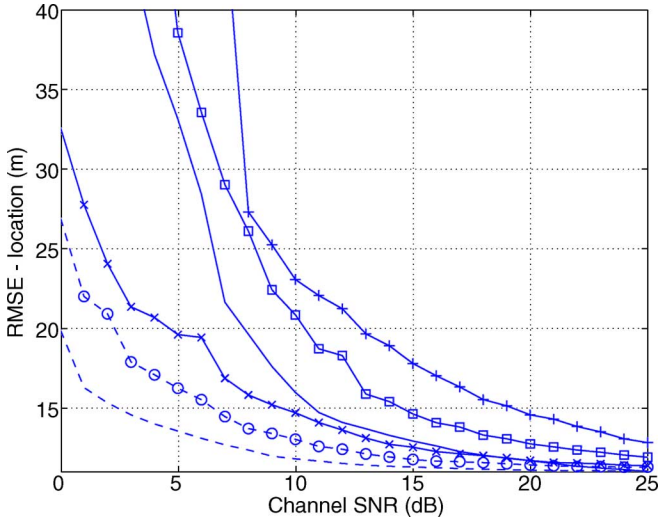

Fig. 9. RMS errors of channel-aware ML estimation methods for different average channel SNRs. Dash line: coherent soft-decoding link, dash-circle: coherent hard-decoding link with channel-aware processing, solid-cross: coherent hard-decoding link with channel-unaware processing, solid: noncoherent soft-decoding link, solid-square: noncoherent hard-decoding link with channel-aware processing, solid-plus: noncoherent hard-decoding link with channel-unaware processing ($\mathrm{N} = 100, \gamma_1 = 1.7, (x_t, y_t) = (10, 20)$).

Proof: See Appendix D. ■

Note that noncoherent reception for a Rayleigh fading hard-decoding link results in a binary nonsymmetric channel model. We should also state that the BER vs. SNR curve obtained using (37) matches the curve obtained by Monte Carlo simulations.

Fig. 9 gives the RMS errors of target location estimates for six different link layer designs with respect to average channel SNR. It is clear from the figure that coherent receivers outperform noncoherent receivers in terms of localization performance no matter which decoding scheme and/or processing algorithm is used. It is interesting to see that the performance of the coherent hard-decoding link with channel-aware and channel-unaware approach is always better than that of all noncoherent link layer designs including soft-decoding and hard-decoding links with channel-aware processing. Furthermore, the performance degradation caused by noncoherent reception is more significant for small SNR values. As can be seen from the figure, noncoherent hard-decoding link with channel-unaware approach requires a much higher SNR value to reach its asymptotic performance compared to other link layer designs. This result indicates that if the employed receiver is noncoherent, channel-aware processing is crucial for good performance even when the channel SNR is relatively high. Since coherent receivers are more expensive to build and operate, a design choice can be made to optimize the performance depending on the channel conditions, available resources and tolerable RMS errors for a specific target localization application. It is also important to note that soft-decoding schemes always perform better than the corresponding hard-decoding schemes, which would not be possible without a channel-aware approach. Using channel statistics in the localization algorithm allows us to use soft-decoding link designs resulting in improved performance without adding any additional communication cost.

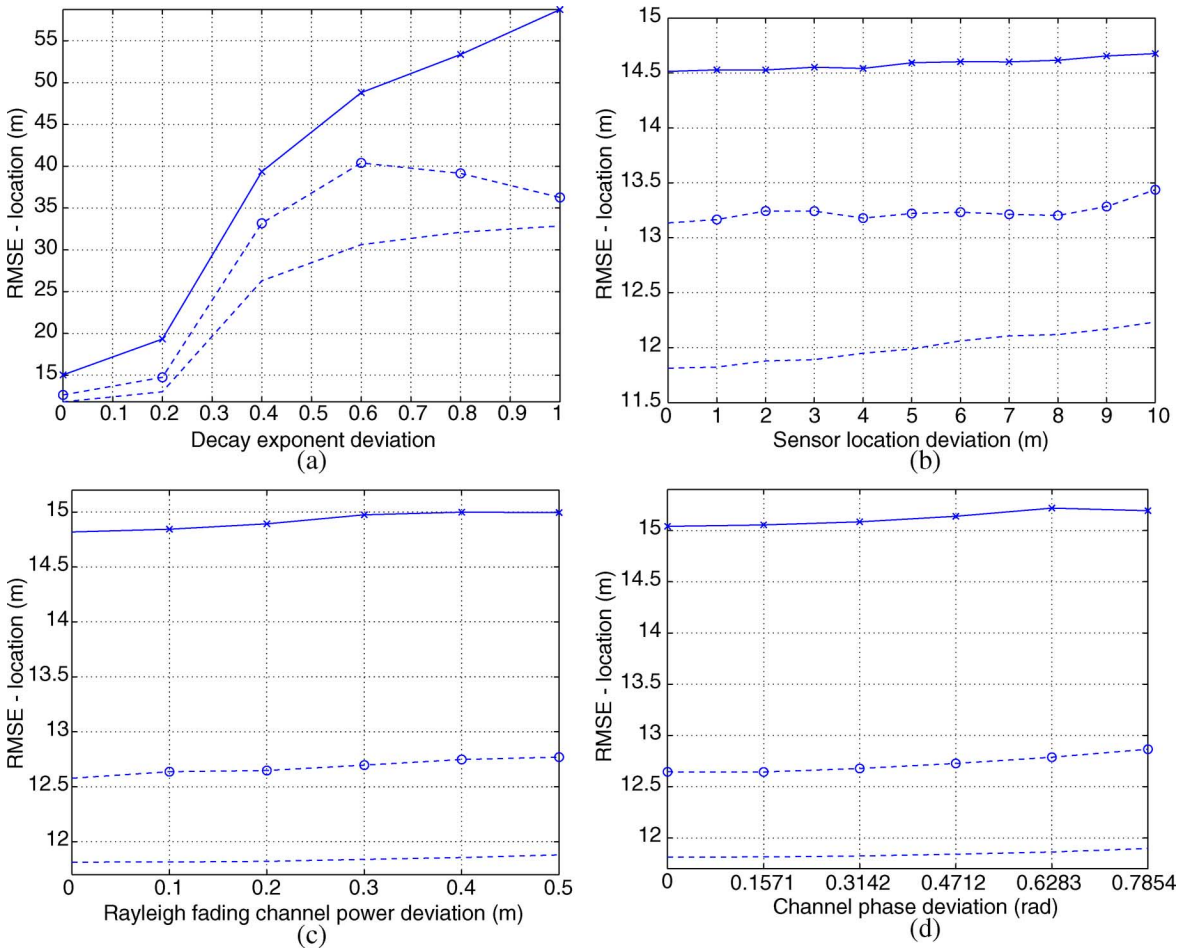

Fig. 10. Dash line: coherent soft-decoding link, dash-circle: coherent hard-decoding link with channel-aware processing, solid-cross: coherent hard-decoding link with channel-unaware processing ($\mathrm{N} = 100, \gamma_1 = 1.7, (x_t, y_t) = (10, 20)$).

D. Sensitivity Analysis

Since the mismatches in the assumed prior information can affect the localization performance, we carry out a sensitivity analysis to analyze the robustness of the developed localization algorithms. The number sensors, N, is set to 100. We consider only the coherent reception case where we keep the nominal parameters the same as in Section IV-B, and simulate the effects of deviations from the nominal values of four different parameters, namely the signal decay exponent (n), sensor locations $((x_i, y_i))$, Rayleigh fading channel power $(E[h_i^2])$ and the channel phase (ϕ_i), for $i = 1, \ldots, N$. The deviation is assumed to be uniformly distributed in the interval 2δ centered at the true values. δ is considered to be $0, 0.2, \ldots, 1$ for the signal decay exponent, $0, 1, \ldots, 10$ for sensor locations, $0, 0.1, \ldots, 0.5$ for Rayleigh fading channel power and $0, (\pi/20), \ldots, (\pi/4)$ for the channel phase. The results are illustrated in Figs. 10(a)–10(d). Results in Fig. 10(a) suggest that the value of the signal decay exponent (n) should be determined very accurately for an acceptable localization performance. Figs. 10(b)–10(d) show that our developed channel aware algorithms are quite robust to errors in sensor locations, Rayleigh fading channel statistics and channel phase mismatches. Robustness to errors in sensor locations is due to the fact that quantized sensor observations are used in the localization process and the number of sensors is large enough to mitigate the effects of sensor location errors. The results in Fig. 10(c), 10(d) are highly encouraging because they show that channel model mismatches do not have any significant effect on the performance of our developed channel aware location estimation algorithms. Robustness of our algorithms to channel statistics as well as the channel phases can be explained by the diversity gained by employing a large number of sensors.

V. Summary and Discussion

In this paper, the target localization problem using a resource constrained WSN with imperfect wireless channels was studied. We have developed a new target localization approach based on ML estimation called channel-aware target localization, which incorporates wireless channel information as well as decoding scheme characteristics at the receiver, and uses quantized sensor data. Three different ML target location estimators have been developed for different link layer designs, namely hard-decoding link modeled as a BC, Rayleigh fading coherent soft-decoding link and Rayleigh fading noncoherent soft-decoding link. In addition, we have derived CRLBs for the developed channel-aware ML estimators and showed that the performance of the estimators converges to their CRLBs even with a relatively small number of sensors. We have also

performed a comparison between channel-aware ML estimators for various link layer designs in order to observe the effects of physical layer parameters on the localization performance. This type of comparison is useful at the design stage and can be utilized to design parameters and functions of the physical layer to optimize performance. Simulation results demonstrate that coherent reception schemes perform better than noncoherent reception schemes for both soft-decoding and hard-decoding links. Furthermore, channel-aware target localization approach makes it possible to employ soft-decoding links at the receiver resulting in improved performance over corresponding hard-decoding links with no additional communication cost. We have also shown by simulations that our channel-aware target localization approach is quite robust to mismatches between the physical system parameters (sensor locations, channel statistics and channel phase) and the assumed system parameters at the fusion center. Our work in this paper is the first step towards considering the WSN system as a whole to optimize the performance of a target localization application. We show here that the physical layer of the network and the localization algorithm at the fusion center should be designed jointly for better localization performance.

Design of optimal local sensor thresholds to improve localization performance is an important problem that needs to be addressed. Additional physical layer parameters and functions other than receiver characteristics such as different modulation and coding schemes can also be incorporated in the localization algorithm to increase the number of dimensions for performance optimization. Furthermore, generalization of the developed channel aware localization algorithms to the multiple target case is another extension that needs to be carried out.

APPENDIX A
PROOF OF THEOREM 1

It is already known that the elements of FIM of a vector parameter θ are defined as

$$[F(\theta)]_{ij} = -E\left[\frac{\partial^2 \ln p(\mathbf{Y}|\theta)}{\partial\theta_i \partial\theta_j}\right]. \tag{40}$$

We first derive the (1,1) element of F. By using (10), we have

$$\frac{\partial \ln p(\mathbf{Y}|\theta)}{\partial P_0} = \sum_{i=1}^{N} \frac{1}{p(\tilde{m}_i|\theta)} \frac{\partial p(\tilde{m}_i|\theta)}{\partial P_0} \tag{41}$$

$$\frac{\partial^2 \ln p(\mathbf{Y}|\theta)}{\partial P_0^2} = \sum_{i=1}^{N} -\frac{1}{p^2(\tilde{m}_i|\theta)} \left[\frac{\partial p(\tilde{m}_i|\theta)}{\partial P_0}\right]^2 + \frac{1}{p(\tilde{m}_i|\theta)} \frac{\partial^2 p(\tilde{m}_i|\theta)}{\partial P_0^2}. \tag{42}$$

Now, the negative expectation is calculated with respect to $p(\tilde{m}_i|\theta)$:

$$\begin{aligned} &-E\left[\frac{\partial^2 \ln p(\mathbf{Y}|\theta)}{\partial P_0^2}\right] \\ &= \sum_{i=1}^{N} \sum_{\tilde{m}_i=0}^{L-1} -p(\tilde{m}_i|\theta) \left\{ -\frac{1}{p^2(\tilde{m}_i|\theta)} \left[\frac{\partial p(\tilde{m}_i|\theta)}{\partial P_0}\right]^2 \right. \\ &\qquad \left. + \frac{1}{p(\tilde{m}_i|\theta)} \frac{\partial^2 p(\tilde{m}_i|\theta)}{\partial P_0^2} \right\} \\ &= \sum_{i=1}^{N} \sum_{\tilde{m}_i=0}^{L-1} \left\{ \frac{1}{p(\tilde{m}_i|\theta)} \left[\frac{\partial p(\tilde{m}_i|\theta)}{\partial P_0}\right]^2 - \frac{\partial^2 p(\tilde{m}_i|\theta)}{\partial P_0^2} \right\}. \end{aligned} \tag{43}$$

The second term in (43) is

$$\sum_{i=1}^{N} \sum_{\tilde{m}_i=0}^{L-1} \frac{\partial^2 p(\tilde{m}_i|\theta)}{\partial P_0^2} = \sum_{i=1}^{N} \frac{\partial^2}{\partial P_0^2} \left[\sum_{\tilde{m}_i=0}^{L-1} p(\tilde{m}_i|\theta)\right] = 0 \tag{44}$$

since $\sum_{\tilde{m}_i=0}^{L-1} p(\tilde{m}_i|\theta) = 1$. Therefore, the expectation reduces to

$$-E\left[\frac{\partial^2 \ln p(\mathbf{Y}|\theta)}{\partial P_0^2}\right] = \sum_{i=1}^{N} \sum_{\tilde{m}_i=0}^{L-1} \frac{1}{p(\tilde{m}_i|\theta)} \left[\frac{\partial p(\tilde{m}_i|\theta)}{\partial P_0}\right]^2. \tag{45}$$

It is easy to see that the partial derivative term in (45) is

$$\frac{\partial p(\tilde{m}_i|\theta)}{\partial P_0} = \sum_{m_i=0}^{L-1} p(\tilde{m}_i|m_i) \frac{\partial p(m_i|\theta)}{\partial P_0}. \tag{46}$$

We derive the following in a straightforward manner

$$\frac{\partial Q\left(\frac{\gamma_{il}-a_i}{\sigma_n}\right)}{\partial P_0} = \frac{d_i^{-\frac{n}{2}}}{2\sqrt{2\pi}\sigma_n\sqrt{P_0}} e^{\frac{-(\gamma_{il}-a_i)^2}{2\sigma_n^2}}. \tag{47}$$

As the conditional PDF $p(m_i|\theta)$ in (5) is composed of $Q(\cdot)$ functions, we can use (47) to obtain

$$\begin{aligned} \frac{\partial p(m_i = l|\theta)}{\partial P_0} &= \frac{\partial}{\partial P_0}\left[Q\left(\frac{\gamma_{il}-a_i}{\sigma_n}\right) - Q\left(\frac{\gamma_{i(l+1)}-a_i}{\sigma_n}\right)\right] \\ &= \frac{d_i^{-\frac{n}{2}}}{2\sqrt{2\pi}\sigma_n\sqrt{P_0}} \\ &\quad \times \left[e^{\frac{-(\gamma_{il}-a_i)^2}{2\sigma_n^2}} - e^{\frac{-\left(\gamma_{i(l+1)}-a_i\right)^2}{2\sigma_n^2}}\right]. \end{aligned} \tag{48}$$

Following a similar procedure, it is easy to derive other elements of the FIM. The derivation is skipped here for the sake of brevity.

APPENDIX B
PROOF OF THEOREM 2

We first derive the (1,1) element of F. By using (25), we have the same expressions as in (41) and (42). Taking the negative expectation and following a similar procedure as in Appendix A, we have

$$-E\left[\frac{\partial^2 \ln p(\mathbf{Y}|\theta)}{\partial P_0^2}\right] = \sum_{i=1}^{N} \int_{-\infty}^{\infty} \left(\frac{1}{p(\tilde{m}_i|\theta)} \left[\frac{\partial p(\tilde{m}_i|\theta)}{\partial P_0}\right]^2 - \frac{\partial^2 p(\tilde{m}_i|\theta)}{\partial P_0^2}\right) d\tilde{m}_i. \tag{49}$$

Note that (49) utilizes the fact that received observation $\tilde{m}_i$ is a real number and can take any value in $(-\infty, \infty)$ for the coherent soft-decoding scheme. Similar to the derivation in Appendix A, the second term in (49) vanishes since

$$\int_{-\infty}^{\infty} \frac{\partial^2 p(\tilde{m}_i|\theta)}{\partial P_0^2} d\tilde{m}_i = \frac{\partial^2}{\partial P_0^2}\left[\int_{-\infty}^{\infty} p(\tilde{m}_i|\theta) d\tilde{m}_i\right] = 0. \tag{50}$$

Therefore, the final expectation is of the form

$$-E\left[\frac{\partial^2 \ln p(\mathbf{Y}|\theta)}{\partial P_0^2}\right]=\sum_{i=1}^{N}\int_{-\infty}^{\infty}\frac{1}{p(\tilde{m}_i|\theta)}\left[\frac{\partial p(\tilde{m}_i|\theta)}{\partial P_0}\right]^2 d\tilde{m}_i \tag{51}$$

where the first term, $p(\tilde{m}_i|\theta)$ has been provided by (24) and the second term is given as

$$\frac{\partial p(\tilde{m}_i|\theta)}{\partial P_0}=\sum_{m_i\in\{-1,1\}} p(\tilde{m}_i|m_i)\frac{\partial p(m_i|\theta)}{\partial P_0}. \tag{52}$$

Note that $\partial p(m_i|\theta)/\partial P_0$ in (52) has been derived in Appendix A.

Other elements of the FIM can be derived easily following a similar procedure. The derivation is skipped here for the sake of brevity.

Appendix C
Proof of Theorem 3

We first derive the (1,1) element of F. Following the same procedures as in Appendices A–B, we have the final expression for the negative expectation

$$-E\left[\frac{\partial^2 \ln p(\mathbf{Y}|\theta)}{\partial P_0^2}\right]=\sum_{i=1}^{N}\int_{0}^{\infty}\frac{1}{p(\tilde{m}_i|\theta)}\left[\frac{\partial p(\tilde{m}_i|\theta)}{\partial P_0}\right]^2 d\tilde{m}_i \tag{53}$$

where the fact that $\tilde{m}_i=|r_i|^2\in[0,\infty)$ has been used. Similarly, the expressions for the terms in the integration are already derived in Section III-C and Appendix A, and other terms of the FIM can be derived following the same procedure. The derivation is skipped here for the sake of brevity.

Appendix D
Proof of Lemma 1

The problem can be set as a binary hypotheses testing problem for ON/OFF signaling in which the signal-plus-noise hypothesis $(\mathcal{H}_1)$ is tested against a noise-only hypothesis $(\mathcal{H}_0)$. Omitting the time and the sensor index, let y denote the received sensor observation. Then

$$\mathcal{H}_1: y=he^{j\phi}B+v$$
$$\mathcal{H}_0: y=v$$

where $he^{j\phi}\sim\mathcal{CN}(0,2\sigma_h^2)$ and $v\sim\mathcal{CN}(0,N_0)$. Note that $N_0=2\sigma_v^2$. Hence, the distribution for both hypotheses can be written as

$$\mathcal{H}_1: y\sim\mathcal{CN}\left(0,2\sigma_h^2B^2+N_0\right)$$
$$\mathcal{H}_0: y\sim\mathcal{CN}(0,N_0). \tag{54}$$

Then, assuming equal prior probabilities $(P(\mathcal{H}_0)=P(\mathcal{H}_1)=1/2)$, the likelihood-ratio (LR) can be expressed as

$$\frac{\frac{1}{\pi\left(2\sigma_h^2B^2+N_0\right)}exp\left(\frac{-|y|^2}{2\sigma_h^2B^2+N_0}\right)}{\frac{1}{\pi N_0}exp\left(\frac{-|y|^2}{N_0}\right)}\underset{H_0}{\overset{H_1}{\gtrless}}1. \tag{55}$$

After taking the logarithm of both sides and some manipulations, the test statistics is obtained as follows:

$$|y|^2\underset{H_0}{\overset{H_1}{\gtrless}}\frac{N_0\left(2\sigma_h^2B^2+N_0\right)}{2\sigma_h^2B^2}\ln\left[\frac{2\sigma_h^2B^2+N_0}{N_0}\right]. \tag{56}$$

Note that the test statistics $|y|^2$ is, in essence, the energy of the received symbol, therefore the corresponding detector is called the energy detector (ED). The expression on the right-hand side of (56) is the detection threshold, which can be represented as γ. Since y is complex Gaussian distributed, it is easy to derive the conditional PDFs

$$p\left(|y|^2|\mathcal{H}_1\right)=\frac{1}{2\sigma_h^2B^2+N_0}exp\left(\frac{-|y|^2}{2\sigma_h^2B^2+N_0}\right) \tag{57}$$

$$p\left(|y|^2|\mathcal{H}_0\right)=\frac{1}{N_0}exp\left(\frac{-|y|^2}{N_0}\right). \tag{58}$$

Then, the error probability is given by

$$\begin{aligned}P_e&=P(decide\ B|\mathcal{H}_0)\frac{1}{2}+P(decide\ 0|\mathcal{H}_1)\frac{1}{2}\\&=P(|y|^2>\gamma|\mathcal{H}_0)\frac{1}{2}+P\left(|y|^2<\gamma|\mathcal{H}_1\right)\frac{1}{2}\end{aligned} \tag{59}$$

which can be calculated with straightforward integration of (57) and (58) to obtain

$$P\left(|y|^2>\gamma|\mathcal{H}_0\right)=\left(\frac{1}{2SNR+1}\right)^{\frac{2SNR+1}{2SNR}} \tag{60}$$

$$P\left(|y|^2<\gamma|\mathcal{H}_1\right)=1-\left(\frac{1}{2SNR+1}\right)^{\frac{1}{2SNR}} \tag{61}$$

resulting in

$$P_e=\frac{1}{2}\left[1-\frac{2SNR}{(2SNR+1)^{\frac{2SNR+1}{2SNR}}}\right] \tag{62}$$

where the average channel SNR is defined as $SNR=(B^2/2N_0)\overline{h^2}$, in which $\overline{h^2}=2\sigma_h^2$.

References

[1] Y. Hu and D. Li, "Energy-based collaborative source localization using acoustic micro-sensor array," *EURASIP J. Appl. Signal Process.*, vol. 2003, no. 4, pp. 321–337, 2003.

[2] T. Pham, B. M. Sadler, and H. Papadopulos, "Energy-based source localization via ad-hoc acoustic sensor network," in *Proc. IEEE Workshop on Statist. Signal Process.*, St. Louis, MO, Sep. 2003, vol. 5, pp. 387–390.

[3] C. Meesookho, U. Mitra, and S. Narayanan, "On energy-based acoustic source localization for sensor networks," *IEEE Trans. Signal Process.*, vol. 56, no. 1, pp. 365–377, Jan. 2008.

[4] M. Z. Rahman, G. C. Karmakar, and L. S. Dooley, "Passive source localization using power spectral analysis and decision fusion in wireless distributed sensor networks," in *Proc. Int. Conf. Inf. Technol.: Coding and Computing (ITCC2005)*, Las Vegas, NV, April 2005, pp. 260–264.

[5] L. M. Kaplan, L. Qiang, and N. Molnar, "Maximum likelihood methods for bearings-only target localization," in *Proc. Int. Conf. Acoust., Speech, Signal Process. (ICASSP2001)*, Salt Lake City, UT, May 2001, vol. 5, pp. 3001–3004.

[6] X. Sheng and Y. Hu, "Energy based acoustic source localization," in *Proc. Int. Workshop on Inf. Process. Sens. Netw.*, Palo Alto, CA, Apr. 2003, pp. 285–300.

[7] X. Sheng and Y. Hu, "Maximum likelihood multiple-source localization using acoustic energy measurements with wireless sensor networks," *IEEE Trans. Signal Process.*, vol. 53, no. 1, pp. 44–53, Jan. 2005.
[8] C. Meesookho and S. Narayanan, "Distributed range difference based target localization in sensor network," in *Proc. Asilomar Conf. Signals, Syst. Comput.*, Pacific Grove, CA, Oct. 2005, pp. 205–209.
[9] R. Niu and P. K. Varshney, "Target location estimation in wireless sensor networks using binary data," in *Proc. Ann. Conf. Inf. Sci. Syst. (CISS2004)*, Princeton, NJ, Mar. 2004.
[10] R. Niu and P. K. Varshney, "Target location estimation in sensor networks with quantized data," *IEEE Trans. Signal Process.*, vol. 54, no. 12, pp. 4519–4528, Dec. 2006.
[11] N. Katenka, E. Levina, and G. Michailidis, Robust Target Localization From Binary Decisions in Wireless Sensor Networks Dep. Statist., Univ. Mich., Tech. Report 452, March 2007.
[12] H. Shi, X. Li, Y. Shang, and D. Ma, "Cramer-Rao bound analysis of quantized RSSI based localization in wireless sensor networks," in *Proc. Intl. Conf. Parallel and Distrib. Syst.*, Fukuoka, Japan, Jul. 2005.
[13] B. Chen, R. Jiang, T. Kasetkasem, and P. K. Varshney, "Channel aware decision fusion in wireless sensor networks," *IEEE Trans. Signal Process.*, vol. 52, no. 12, pp. 3454–3458, Dec. 2004.
[14] B. Chen and P. K. Willett, "On the optimality of the likelihood-ratio test for local sensor decision rules in the presence of nonideal channels," *IEEE Trans. Inf. Theory*, vol. 51, no. 2, pp. 693–699, Feb. 2005.
[15] R. Jiang and B. Chen, "Fusion of censored decisions in wireless sensor networks," *IEEE Trans. Wireless Commun.*, vol. 4, no. 6, pp. 2668–2673, Nov. 2005.
[16] R. Niu, B. Chen, and P. K. Varshney, "Fusion of decisions transmitted over Rayleigh fading channels in wireless sensor networks," *IEEE Trans. Signal Process.*, vol. 54, no. 3, pp. 1018–1027, March 2006.
[17] B. Chen, L. Tong, and P. K. Varshney, "Channel-aware distributed detection in wireless sensor networks," *IEEE Signal Process. Mag. (Special Issue on Distrib. Signal Process. Sens. Netw.)*, vol. 23, pp. 16–26, Jul. 2006.
[18] B. Liu and B. Chen, "Channel optimized quantizers for decentralized detection in wireless sensor networks," *IEEE Trans. Inf. Theory*, vol. 52, no. 7, pp. 3349–3358, July 2006.
[19] Q. Cheng, B. Chen, and P. K. Varshney, "Detection performance limits for distributed sensor networks in the presence of nonideal channels," *IEEE Trans. Wireless Commun.*, vol. 5, no. 11, pp. 3034–3038, Nov. 2006.
[20] O. Ozdemir, R. Niu, and P. K. Varshney, "Channel aware target localization in wireless sensor networks," in *Proc. Int. Conf. Inf. Fusion (Fusion 2007)*, Quebec City, Canada, Jul. 2007.
[21] S. M. Kay, *Fundamentals of Statistical Signal Processing, Vol:II—Estimation Theory*. Upper Saddle River, NJ: Prentice-Hall, 1993.
[22] T. D. Rappoport, *Wireless Communications-Priciples and Practices*. Upper Saddle River, NJ: Prentice-Hall, 1996.
[23] D. Tse and P. Viswanath, *Fundamentals of Wireless Communication*. Cambridge, U.K.: Cambridge Univ. Press, 2005.
[24] E. Biglieri, R. Calderbank, A. Constantinides, A. Goldsmith, A. Paulraj, and H. V. Poor, *MIMO Wireless Communications*. Cambridge: Cambridge Univ. Press, 2007.
[25] J. H. Mathews and K. K. Fink, *Numerical Methods Using Matlab*, 4th ed. Upper Saddle River, NJ: Prentice-Hall, 2004.

Onur Ozdemir (S'06) was born in Ankara, Turkey, on March 4, 1980. He received the B.S. degree in electrical and electronics engineering from Bogazici University, Istanbul, Turkey, in 2003, and the M.S. degree in electrical engineering from Syracuse University, Syracuse, NY, in 2004.

Since 2004, he has been pursuing the Ph.D. degree in electrical engineering at Syracuse University. He was an intern at Mitsubishi Electric Research Laboratories, Cambridge, MA, in 2007 and 2009. His research interests are in the areas of statistical signal processing, data fusion, and their applications to sensor networks and wireless communications.

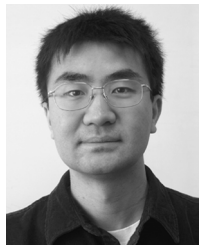

Ruixin Niu (M'04) received the B.S. degree from Xi'an Jiaotong University, Xi'an, China, in 1994, the M.S. degree from the Institute of Electronics, Chinese Academy of Sciences, Beijing, in 1997, and the Ph.D. degree from the University of Connecticut, Storrs, in 2001, all in electrical engineering.

He is currently a Research Assistant Professor with Syracuse University, Syracuse, NY. His research interests are in the areas of statistical signal processing and its applications, including detection, estimation, data fusion, communications, and image processing.

Dr. Niu received the Fusion 2004 Best Paper Award in the Seventh International Conference on Information Fusion, Stockholm, Sweden, in June 2004.

Pramod K. Varshney (F'97) was born in Allahabad, India, on July 1, 1952. He received the B.S. degree in electrical engineering and computer science (with highest honors) and the M.S. and Ph.D. degrees in electrical engineering from the University of Illinois at Urbana-Champaign in 1972, 1974, and 1976, respectively.

Since 1976, he has been with the Electrical and Computer Engineering Department, Syracuse University, Syracuse, NY, where he is currently a Distinguished Professor of electrical engineering and computer science. His current research interests are in distributed sensor networks and data fusion, detection and estimation theory, wireless communications, image processing, radar signal processing, and remote sensing. He has published extensively. He is the author of *Distributed Detection and Data Fusion* (New York: Springer-Verlag, 1997).

Dr. Varshney was a James Scholar, a Bronze Tablet Senior, and a Fellow while with the University of Illinois. He is a member of Tau Beta Pi and is the recipient of the 1981 ASEE Dow Outstanding Young Faculty Award. He was the Guest Editor of the Special Issue on Data Fusion of the PROCEEDINGS OF THE IEEE, January 1997. In 2000, he received the Third Millennium Medal from the IEEE and Chancellor's Citation for Exceptional Academic Achievement at Syracuse University. He serves as a Distinguished Lecturer for the AES Society of the IEEE. He is on the editorial boards of the *International Journal of Distributed Sensor Networks* and the IEEE TRANSACTIONS ON SIGNAL PROCESSING. He was the President of the International Society of Information Fusion during 2001.